Inorg. Chem. **2002**, *41*, 1920–1929

Effect of Metal–Oxygen Covalent Bonding on the Competition between Jahn–Teller Distortion and Charge Disproportionation in the Perovskites of High-Spin d^4 Metal Ions $LaMnO_3$ and $CaFeO_3$

M.-H. Whangbo* and H.-J. Koo

Department of Chemistry, North Carolina State University, Raleigh, North Carolina 27695-8204

A. Villesuzanne and M. Pouchard*

ICMCB-CNRS, 87 avenue du Dr. A. Schweitzer, 33608 Pessac Cedex, France

Received October 9, 2001

The perovskites $LaMnO_3$ and $CaFeO_3$ consisting of high-spin d^4 transition metal ions undergo different types of distortions, i.e., a Jahn–Teller distortion in $LaMnO_3$ and a charge disproportionation in $CaFeO_3$. We investigated the electronic factor causing this difference on the basis of first principles spin-polarized electronic band structure calculations for their ideal cubic structures and also tight-binding electronic band structure calculations for their ideal cubic and distorted structures. Our study shows that a charge disproportionation is favored over a Jahn–Teller distortion in $CaFeO_3$ because the covalent character is strong in the Fe–O bond, while the opposite is true for $LaMnO_3$ because the covalent character is weak in the Mn–O bond. In spin-polarized electronic band structure calculations, the covalency of the M–O (M = Fe, Mn) bond is enhanced in the up-spin bands but is reduced in the down-spin bands. Our analysis shows that electron–electron repulsion causes the energy gap between the metal 3d and the oxygen 2p orbitals to become larger for the down-spin than for the up-spin–orbital interactions. Thus in the d-block e_g bands of both $LaMnO_3$ and $CaFeO_3$ the metal 3d orbital contribution is larger in the down-spin than in the up-spin bands.

1. Introduction

In transition metal perovskites AMO_3 (A = alkaline earth, rare earth; M = transition metal), the A^{n+} cations ($n = 2, 3$) occupy the 12-coordinate sites of the three-dimensional lattice made up of corner-sharing MO_6 octahedra. The relative arrangement of the MO_6 octahedra in AMO_3 is governed largely by the tolerance factor $\tau = r_{A-O}/\sqrt{2}r_{M-O}$ defined by the A−O and M−O distances.[1,2] In the ideal cubic structure for which $\tau = 1$, the M−O−M bridge is linear (Figure 1a). With a small A^{n+} cation for which $\tau < 1$, the ideal cubic structure becomes unstable because the 12-coordinate site is larger in size than the A^{n+} cation. Such a perovskite reduces the size of the 12-coordinate site by cooperatively tilting the MO_6 octahedra and bending the M−O−M bridges. Thus, the resulting structure deviates from the ideal cubic structure, as found for example in $LaMnO_3$[3−5] and $CaFeO_3$[6,7] (Figure 1b). Another important structural feature of a perovskite is a distortion in the individual MO_6 octahedra. The Mn^{3+} ions of $LaMnO_3$ have the high-spin d^4 configuration, $(t_{2g})^3(e_g)^1$,[8] so each MnO_6 octahedron is subject to a Jahn−Teller (JT) distortion that lifts the degeneracy of the e_g level.[9] Indeed the MnO_6 octahedra of $LaMnO_3$ undergo a JT distortion in a cooperative manner.[3−5] The perovskite $CaFeO_3$ is isoelectronic with $LaMnO_3$ and the Fe^{4+} ion has the high-spin d^4 configuration, $(t_{2g})^3(e_g)^1$,[10] so that $CaFeO_3$ should also possess JT instability. However, $CaFeO_3$ does not show a JT distortion but undergoes a charge dispropor-

* To whom correspondence should be addressed. E-mail (M.-H.W.): mike_whangbo@ncsu.edu.

(1) Goodenough, J. B.; Zhou, J.-S. *Chem. Mater*. **1998**, *10*, 2980.
(2) Goodenough, J. B. *Struct. Bonding* **2001**, *98*, 1.
(3) Norby, P.; Krogh Andersen, I. G.; Krogh Andersen, E.; Andersen, N. H. *J. Solid State Chem*. **1995**, *119*, 191.
(4) Elemans, J. B. A. A.; Van Laar, B.; Van Der Veen, K. R.; Loopstra, B. O. *J. Solid State Chem*. **1971**, *3*, 238.
(5) Alonso, J. A.; Martínez-Lope, M. J.; Casais, M. T.; Fernández-Díaz, M. T. *Inorg. Chem*. **2000**, *39*, 917.
(6) Woodward, P. M.; Cox, D. E.; Moshopoulou, E.; Sleight, A. W.; Morimoto, S. *Phys. Rev. B* **2000**, *62*, 844 and references therein.
(7) Takeda, T.; Kanno, R.; Kawamoto, Y.; Takano, M.; Kawasaki, S.; Kamiyama, T.; Izumi, F. *Solid State Sci*. **2000**, *2*, 673.
(8) Matsumoto, G. *J. Phys. Soc. Jpn*. **1970**, *29*, 606.
(9) Kaplan, M. D.; Vekhter, B. G. *Cooperative Phenomena in Jahn−Teller Crystals*; Plenum: New York, 1995.

10.1021/ic0110427 CCC: $22.00 © 2002 American Chemical Society
Published on Web 03/01/2002

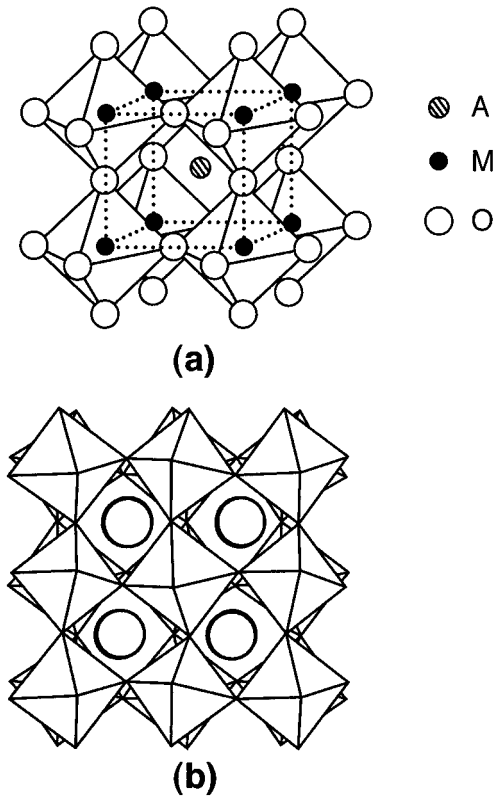

Figure 1. (a) Perspective view of an ideal cubic structure of a perovskite AMO_3. (b) Polyhedral representation of an orthorhombic structure of a perovskite AMO_3.

tionation (CD) of the type $2Fe^{4+} \rightarrow Fe^{(4+\delta)+} + Fe^{(4-\delta)+}$ in varying degrees of δ as a function of temperature.[6,7,10,11]

The absence of a JT distortion in $CaFeO_3$ has been rationalized by considering the electron configuration of Fe^{4+} as d^5L and describing the CD process as $2d^5L \rightarrow d^5 + d^5L^2$.[11] We note that, in the t_{2g}- and e_g-block levels of each MO_6 (M = Mn, Fe) octahedron, the metal 3d and oxygen 2p orbitals have antibonding combinations (π- and σ-type, respectively) and that the ionic configuration d^4 means the electron configuration $(t_{2g})^3(e_g)^1$, i.e., the presence of three electrons in the t_{2g}-block levels and one electron in the e_g-block levels.[12,13] Consequently, the notation d^4 for Fe^{4+} used in the ionic electron counting scheme is equivalent in meaning to the notation d^5L for Fe^{4+} commonly used in describing results of spectroscopic measurements. Consequently, the notational change from d^4 to d^5L for Fe^{4+} does not explain why $CaFeO_3$ undergoes a CD instead of a JT distortion. Since the transition metal ions of $LaMnO_3$ and $CaFeO_3$ have the same electron configuration, i.e., $(t_{2g})^3(e_g)^1$, it is reasonable to suppose that both perovskites are susceptible to a JT distortion as well as a CD. Then the experimental observations imply that JT instability is stronger than CD instability in $LaMnO_3$, while the opposite is true in $CaFeO_3$. In this study, we explore these implications on the basis of electronic band structure calculations for the ideal cubic and distorted structures of $LaMnO_3$ and $CaFeO_3$.

2. Spin-Polarized Electronic Band Structures

Iron is more electronegative than manganese so that the Fe 3d level is closer in energy to the oxygen 2p level than is the Mn 3d level. In addition, La−O bonds are significantly more covalent than Ca−O bonds. Consideration of the inductive effect[14,15] suggests that the Fe−O bonds of $CaFeO_3$ should be more covalent than the Mn−O bonds of $LaMnO_3$ and so does that of the electronegativity difference (see below). (It should be emphasized that the two compounds have an identical metal ion configuration, i.e., $(t_{2g})^3(e_g)^1$. The d-block levels are antibonding in the metal−oxygen bonds, so different electron configurations result in different bond strengths. For compounds with different electron configurations, it would be difficult to compare their bond strengths using the concepts of electronegativity and inductive effect.) To verify this point, we perform first principles electronic band structure calculations for the ideal cubic structures of $LaMnO_3$ and $CaFeO_3$ using the WIEN97 Full Potential Linearized Augmented Plane Wave (FLAPW) program package,[16] within the generalized gradient approximation[17] for the exchange-correlation energy. The ideal cubic structures of $LaMnO_3$ and $CaFeO_3$ were constructed using the average Mn−O and Fe−O distances (1.987 and 1.918 Å, respectively) determined from the distorted structures of $LaMnO_3$ and $CaFeO_3$, respectively. Muffin-tin radii of 2.0 au for La and Ca, 1.9 au for Mn and Fe, and 1.7 au for O were used. The basis sets consisted of 224 and 207 plane waves for $LaMnO_3$ and $CaFeO_3$, respectively ($G_{max} = 10$). Integrations over the irreducible wedge of the Brillouin zone were carried out using a 56 k-points regular mesh. Since the d-electrons of $LaMnO_3$ and $CaFeO_3$ are localized,[8,10] we carry out both non-spin-polarized and spin-polarized electronic band structure calculations. Spin-polarized solutions were found more stable in both cases.

Results of our calculations are summarized in terms of the total density of states (TDOS) and partial density of states (PDOS) plots in Figure 2 for $LaMnO_3$ and in Figure 3 for $CaFeO_3$. The Fermi level of $LaMnO_3$ occurs in the up-spin e_g bands while the down-spin t_{2g} and e_g bands are empty. The Fermi level of $CaFeO_3$ occurs in the up-spin e_g bands and at the bottom of the down-spin t_{2g}. This is in support of the picture that the Mn^{3+} and Fe^{4+} ions of these perovskites have the high-spin $(t_{2g})^3(e_g)^1$ configuration with a small but nonnegligible low-spin admixture in the case of Fe^{4+}. From the viewpoint of the nonmagnetic metallic state, in which the up- and down-spin bands are identical, the unequal occu-

(10) Takano, M.; Nasu, S.; Abe, T.; Yamamoto, K.; Endo, S.; Takeda, Y.; Goodenough, J. B. *Phys. Rev. Lett.* **1991**, *67*, 3267.
(11) Kawasaki, S.; Takano, M.; Kanno, R.; Takeda, T.; Fujimori, A. *J. Phys. Soc. Jpn.* **1998**, *67*, 1529.
(12) Lee, K.-S.; Koo, H.-J.; Dai, D.; Ren, J.; Whangbo, M.-H. *Inorg. Chem.* **1999**, *38*, 340.
(13) Lee, K.-S.; Koo, H.-J.; Ren, J.; Whangbo, M.-H. *J. Solid State Chem.* **1999**, *147*, 11.
(14) Etourneau, J.; Portier, J.; Ménil, F. *Alloys Met.* **1992**, *188*, 1.
(15) Villesuzanne, A.; Pouchard, M. *C. R. Acad. Sci. Paris, Ser. 2* **1996**, *310*, 155.
(16) Blaha, P.; Schwarz, K.; Luitz, J. *WIEN97*; Vienna University of Technology: Vienna, 1997. (Improved and updated version of the original copyrighted WIEN code. See: Blaha, P.; Schwarz, K.; Sorantin, P.; Trickey, S. B. *Comput. Phys. Commun.* **1990**, *59*, 399.)
(17) Perdew, J. P.; Burke, K.; Ernzerhof, M. *Phys. Rev. Lett.* **1996**, *77*, 3865.

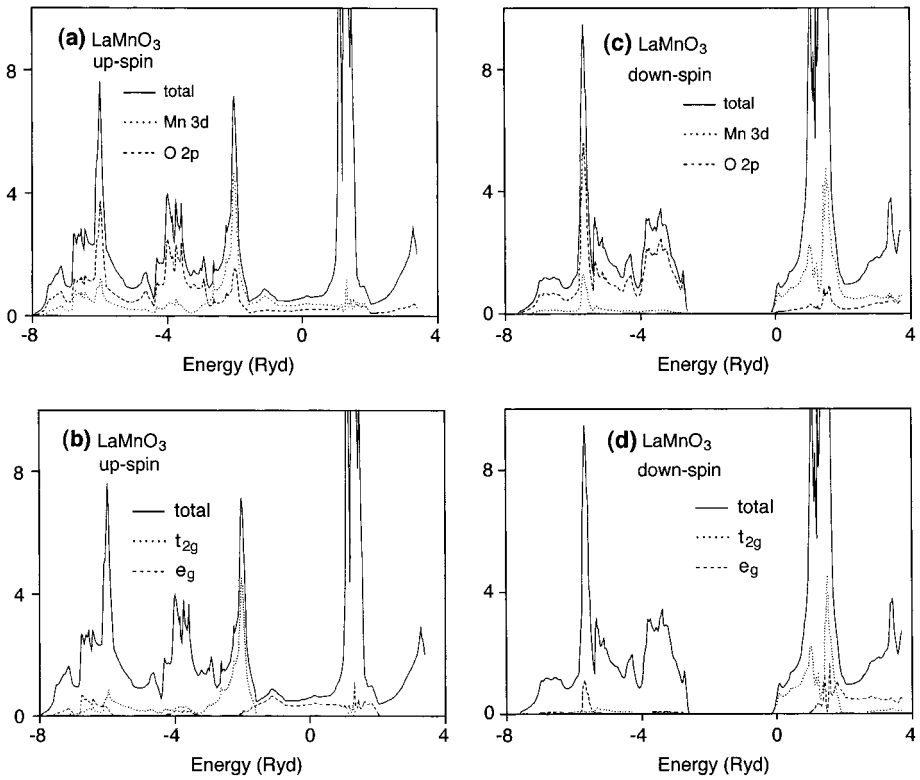

Figure 2. TDOS and PDOS plots calculated for the ideal cubic structure of $LaMnO_3$, where the Fermi level is located at zero. (a) Decomposition of the TDOS (solid line) for the up-spin bands into the Mn atom (dotted line) and oxygen atom (dashed line) contributions. The peak at ~1.6 eV represents the La 4f states. (b) Decomposition of the TDOS (solid line) for the up-spin bands into the t_{2g} orbital (dotted line) and e_g orbital (dashed line) contributions. (c) Decomposition of the TDOS (solid line) for the down-spin bands into the Mn atom (dotted line) and oxygen atom (dashed line) contributions. (d) Decomposition of the TDOS (solid line) for the down-spin bands into the t_{2g} orbital (dotted line) and e_g orbital (dashed line) contributions.

pations of the up- and down-spin bands in the magnetic state are a consequence of lowering the up-spin bands and raising the down-spin bands in energy.[18] In addition to this band shifting, the orbital compositions of the up- and down-spin bands become different somewhat in self-consistent-field electronic band structure calculations. In a spin-polarized FLAPW study of $La_{1-x}Sr_xMnO_3$,[19] it was reported that the covalent character of the Mn−O bond is stronger in the up-spin than in the down-spin bands. Our calculations for $LaMnO_3$ and $CaFeO_3$ show a similar observation. The cause for this phenomenon is discussed in the following.

Let us consider the relative contributions of the transition metal 3d and oxygen 2p orbitals to the up- and down-spin e_g bands, [3d]/[2p]. The metal 3d and oxygen 2p orbitals make σ-antibonding interactions in the transition metal e_g bands, so the [3d]/[2p] ratio provides a qualitative estimate for the degree of covalent bonding in the M−O (M = Mn, Fe) bonds. According to the concept of orbital interaction,[20] the σ-bonding and σ-antibonding orbitals of a highly covalent M−O bond would have almost equal contributions from the metal 3d and oxygen 2p orbitals. When the metal 3d level is raised above the oxygen 2p level, the covalent character of the M−O bond decreases (or the ionic character of the M−O bond increases) and the metal 3d orbital contributes more than does the oxygen 2p orbital to the σ-antibonding level of the M−O bond so that the [3d]/[2p] ratio increases. Thus, the smaller the [3d]/[2p] ratio, the stronger the covalent character of the M−O bond becomes. For $LaMnO_3$ the [3d]/[2p] ratios are in the range of 2 and 4 for the up- and down-spin e_g bands, respectively (Figure 2). For $CaFeO_3$ the [3d]/[2p] ratios are in the range of 1 and 2 for the up- and down-spin e_g bands, respectively (Figure 3). Therefore, the Fe−O bonds of $CaFeO_3$ are more covalent than are the Mn−O bonds of $LaMnO_3$. Furthermore, the Mn−O bonds of $LaMnO_3$ are more covalent in the up-spin than in the down-spin bands, and so are the Fe−O bonds of $CaFeO_3$. The [3d]/[2p] ratio in the up-spin e_g bands of $CaFeO_3$ amounts to a high degree of covalency in transition metal oxides, and this also affects the orbital compositions of the up-spin bands; Figure 3a shows that the density of states cannot be classified into nine O 2p-, three Fe t_{2g}-, and two Fe e_g-block bands but consists of two Fe e_g-block bands plus two groups of six bands that have almost equal contributions of the O 2p and Fe 3d orbitals. The same effect was recently found in the spin-polarized FLAPW calculations for $TlSr_2CoO_5$ and $SrCoO_3$.[21]

3. Effect of Electron−Electron Repulsion on Orbital Mixing

It is important to understand why spin-polarized electronic band structure calculations lead to different orbital composi-

(18) Jung, D.; Koo, H.-J.; Whangbo, M.-H. *J. Mol. Struct. (THEOCHEM)* **2000**, *527*, 113.
(19) Pickett, W. E.; Singh, D. J. *Phys. Rev. B* **1996**, *53*, 1146.
(20) Albright, T. A.; Burdett, J. K.; Whangbo, M.-H. *Orbital Interactions in Chemistry*; Wiley: New York, 1985.
(21) Pouchard, M.; Villesuzanne, A.; Doumerc, J.-P. *J. Solid State Chem.* **2001**, *162*, 282.

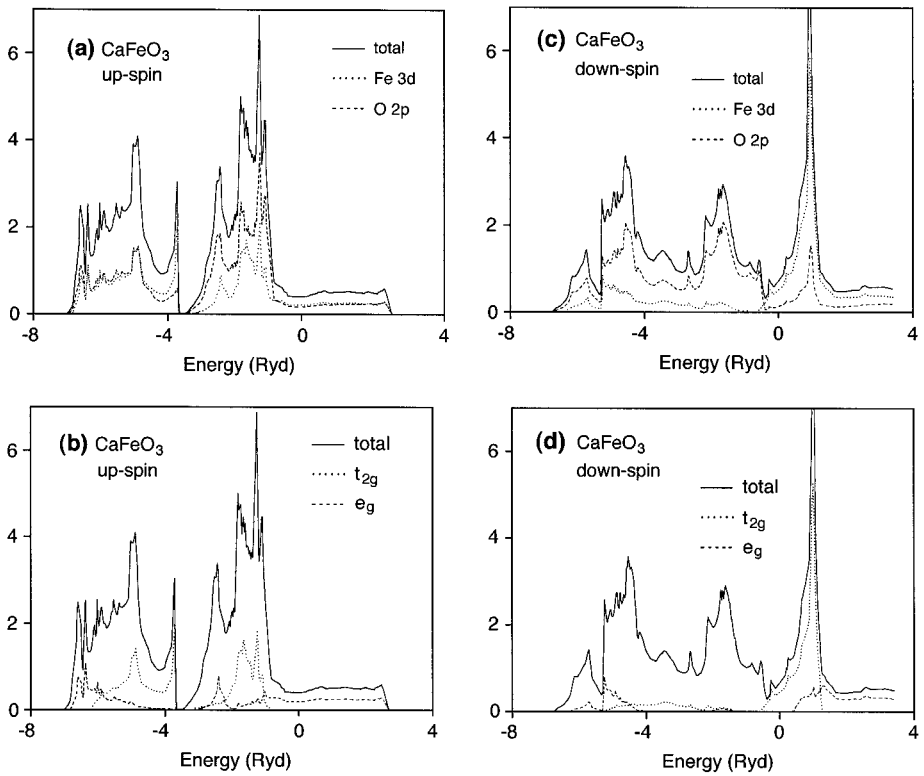

Figure 3. TDOS and PDOS plots calculated for the ideal cubic structure of $CaFeO_3$: (a) decomposition of the TDOS (solid line) for the up-spin bands into the Fe atom (dotted line) and oxygen atom (dashed line) contributions; (b) decomposition of the TDOS (solid line) for the up-spin bands into the t_{2g} orbital (dotted line) and e_g orbital (dashed line) contributions; (c) decomposition of the TDOS (solid line) for the down-spin bands into the Fe atom (dotted line) and oxygen atom (dashed line) contributions; (d) decomposition of the TDOS (solid line) for the down-spin bands into the t_{2g} orbital (dotted line) and e_g orbital (dashed line) contributions.

tions in the up- and down-spin bands of a given compound. In the occupied up-spin e_g bands of $CaFeO_3$, the Fe 3d and the O 2p orbitals contribute almost equally. As already pointed out, this means that the Fe 3d and the O 2p levels are nearly the same for the up-spin bands. In the unoccupied down-spin e_g bands of $CaFeO_3$, the Fe 3d orbital contribution is larger than the O 2p orbital contribution. Thus, the Fe 3d level lies above the O 2p level for the down-spin bands. In the occupied up-spin e_g bands of $LaMnO_3$, the Mn 3d orbital contributes more than does the O 2p orbital. Thus, the Mn 3d level lies above the O 2p level for the up-spin bands. In the unoccupied down-spin e_g bands of $LaMnO_3$, the Mn 3d orbital contribution is much larger than the O 2p orbital contribution. Therefore, the Mn 3d level for the down-spin e_g bands lies higher than that for the up-spin e_g bands. To explain these observations, it is necessary to examine how orbital interactions are affected by electron−electron repulsion and in what way the effect is different for up-spins and down-spins.

From the viewpoint of spin-polarized band structures, the very first effect of electron−electron repulsion is to induce the high-spin $(t_{2g})^3(e_g)^1$ configuration for Mn^{3+} and Fe^{4+}. Thus, as the starting point of our discussion, we consider the energies of metal 3d and oxygen 2p levels in the non-spin-polarized case depicted in Figure 4a, which shows four singly filled 3d-levels of a metal ion and a doubly filled 2p-orbital of a ligand oxygen. In terms of exchange interactions alone, the metal up-spin 3d-level is stabilized by $-3K_{dd}$ and the oxygen up-spin 2p-level by $-4K_{dp}$ with respect to their

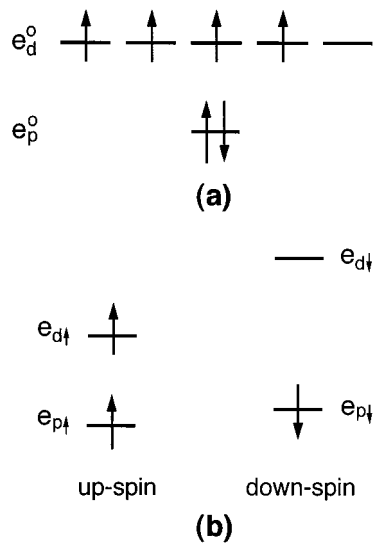

Figure 4. Effect of electron−electron repulsion on the energy gap associated with the orbital interaction of a doubly filled oxygen 2p orbital with partially filled 3d orbitals of a d^4 transition metal cation. The energy levels of the metal 3d and oxygen 2p orbitals are shown (a) in the absence of electron−electron repulsion and (b) in the presence of electron−electron repulsion.

corresponding down-spin levels. (Here K_{dd} is the exchange integral for two electrons on the metal and K_{dp} is the exchange integral for one electron on the metal and one electron on oxygen.) Thus, the energy gap between the metal 3d and oxygen 2p levels is reduced for the up-spin electrons because $K_{dd} \gg K_{dp}$. The primary effect of Coulomb interac-

tions is to raise the energy of the empty down-spin metal 3d level, because this energy is equal to the effective potential exerted to an electron if it were to occupy that orbital.[21−23] This enhances the energy gap between the metal 3d and oxygen 2p levels for the down-spin electrons. In the following we provide a more quantitative description of these qualitative ideas on the basis of Figure 4a.

When electron−electron repulsion is taken into consideration,[21−23] the up- and down-spin levels of the metal 3d and oxygen 2p orbitals are expressed as (Figure 4b)

$$e_{p\uparrow} = e_p^{\,0} + U_{pp} + 4J_{pd} - 4K_{pd}$$

$$e_{d\uparrow} = e_d^{\,0} + 3J_{dd} - 3K_{dd} + 2J_{pd} - K_{pd}$$

$$e_{p\downarrow} = e_p^{\,0} + U_{pp} + 4J_{pd}$$

$$e_{d\downarrow} = e_d^{\,0} + 4J_{dd} + 2J_{pd} - K_{pd} \quad (1)$$

where U_{pp} is the on-site Coulomb repulsion for the oxygen 2p orbital, J_{dd} is the Coulomb repulsion between two different metal 3d-orbitals, and J_{dp} is the Coulomb repulsion between a metal 3d and the oxygen 2p orbital. Therefore, for the up- and down-spin electrons, the energy gaps between the metal 3d and the oxygen 2p levels are written as

$$e_{d\uparrow} - e_{p\uparrow} = (e_d^{\,0} - e_p^{\,0}) + (-3K_{dd} + 3K_{pd}) + (3J_{dd} - U_{pp} - 2J_{pd})$$

$$e_{d\downarrow} - e_{p\downarrow} = (e_d^{\,0} - e_p^{\,0}) + (J_{dd} - K_{pd}) + (3J_{dd} - U_{pp} - 2J_{pd}) \quad (2)$$

Consequently, the energy gap between the metal 3d and the oxygen 2p levels for down-spin electrons is larger than that for the up-spin electrons by

$$(e_{d\downarrow} - e_{p\downarrow}) - (e_{d\uparrow} - e_{p\uparrow}) = J_{dd} + 3K_{dd} - 4K_{pd} \approx U_{dd} + K_{dd} - 4K_{pd} \quad (3)$$

where U_{dd} is the on-site Coulomb repulsion for two electrons in a metal 3d level and is approximately related to J_{dd} and K_{dd} as $J_{dd} \approx U_{dd} - 2K_{dd}$.[21] In general, the magnitudes of the various Coulomb and exchange integrals are expected to decrease as $U_{dd} > U_{pp} > J_{dd} > J_{dp} > K_{dd} > K_{dp}$. It is clear from eq 3 that electron−electron repulsion makes larger the energy gap between the metal 3d and the oxygen 2p levels for the down-spin−orbital interactions than for the up-spin−orbital interactions. This explains why, for both $LaMnO_3$ and $CaFeO_3$, the covalency of the M−O (M = Fe, Mn) bond is greater in the up-spin than in the down-spin bands.

4. Metal−Oxygen Covalent Bonding and Competition between JT and CD Instability

In the d-block bands of $LaMnO_3$ and $CaFeO_3$ (equivalently, in the d-block levels of MnO_6 and FeO_6 octahedra), the metal 3d orbitals make antibonding interactions with the oxygen 2p orbitals. In the ligand p-block levels of MnO_6 and FeO_6 octahedra that have the t_{2g} and e_g symmetries, the oxygen 2p orbitals make bonding interactions with the metal 3d orbitals.[20] Consequently, a more complete description of the high-spin d^4 configuration at each transition metal cation is $(L\text{-}t_{2g}\uparrow)^3(L\text{-}e_g\uparrow)^2(M\text{-}t_{2g}\uparrow)^3(M\text{-}e_g\uparrow)^1$ for the up-spin levels and as $(L\text{-}t_{2g}\downarrow)^3(L\text{-}e_g\downarrow)^2$ for the down-spin levels, where the symbols L and M refer to the ligand p-block and the transition metal d-block, respectively. The L-t_{2g} and L-e_g levels, regardless of whether they refer to up- or down-spin levels, have π- and σ-bonding interactions between the metal 3d and oxygen 2p orbitals. The M-$t_{2g}\uparrow$ and M-$e_g\uparrow$ levels have π- and σ-antibonding interactions between the metal 3d and oxygen 2p orbitals, respectively. The nodal properties of the two L-e_g and two M-e_g levels of an MO_6 octahedron are shown in Figure 5. The σ-interactions are more strongly affected by a change in the M−O bond lengths associated with JT and CD distortions. Therefore, it is sufficient to consider only the σ-interactions in our discussion.

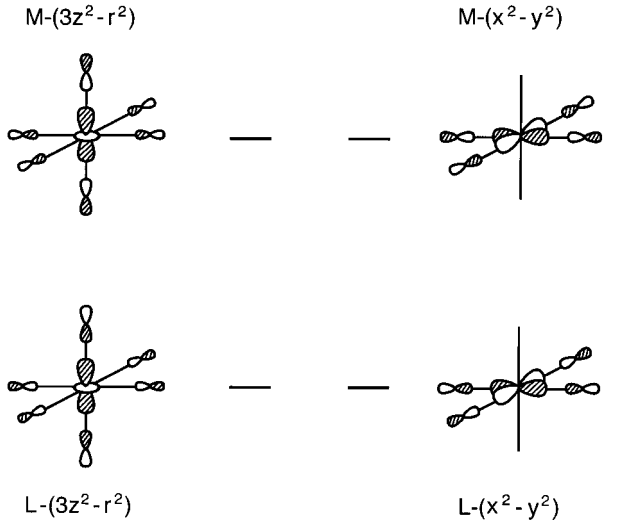

Figure 5. Nodal properties of the two L-e_g and two M-e_g levels of an MO_6 octahedron.

In a cooperative JT distortion of AMO_3 (Figure 6a), each MO_6 octahedron is distorted such that two trans M−O bonds (along the z-direction) increase in length while another two trans M−O bonds (along the *x*-direction) decrease in length. To a first approximation, the remaining two M−O bonds (along the *y*-direction) do not change in length. Each e_g set of orbitals has "$3z^2 - r^2$" and "$x^2 - y^2$" components (Figure 5). Then a JT distortion lowers the M-($3z^2 - r^2$) levels but raises L-($3z^2 - r^2$) levels while it raises the M-($x^2 - y^2$) levels but lowers L-($x^2 - y^2$) levels (Figure 6b,c). During the JT distortion the lowering of the L-($x^2 - y^2$) levels should be significantly smaller in magnitude than the raising of the L-($3z^2 - r^2$) levels because the distortion affects half the M−O bonds in the L-($x^2 - y^2$) levels but all the M−O bonds in the L-($3z^2 - r^2$) levels. For similar reasons, the raising of the M-($x^2 - y^2$) levels should be significantly smaller in magnitude than the lowering of the M-($3z^2 - r^2$) levels. The JT instability in transition metal oxides is commonly discussed by considering how the M-($3z^2 - r^2$) and M-(x^2

(22) Brandow, B. H. *Adv. Phys*. **1977**, *26*, 651.

(23) Whangbo, M.-H. *Inorg. Chem*. **1980**, *19*, 1728.

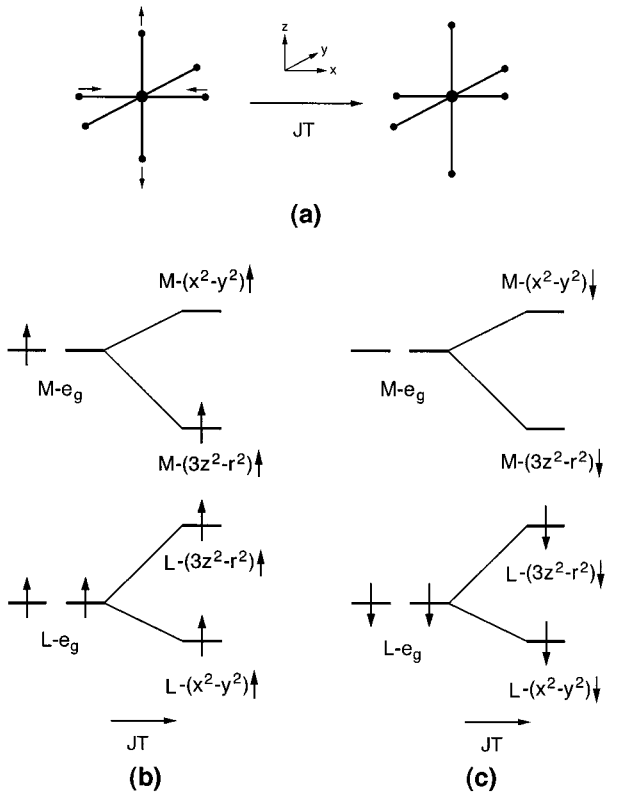

Figure 6. (a) Schematic representation of a JT distortion in a MO_6 octahedron containing a d^4 metal ion. (b) Effect of the JT distortion on the L-$e_g\uparrow$ and M-$e_g\uparrow$ orbitals of an MO_6 octahedron. (c) Effect of the JT distortion on the L-$e_g\downarrow$ and M-$e_g\downarrow$ orbitals of an MO_6 octahedron.

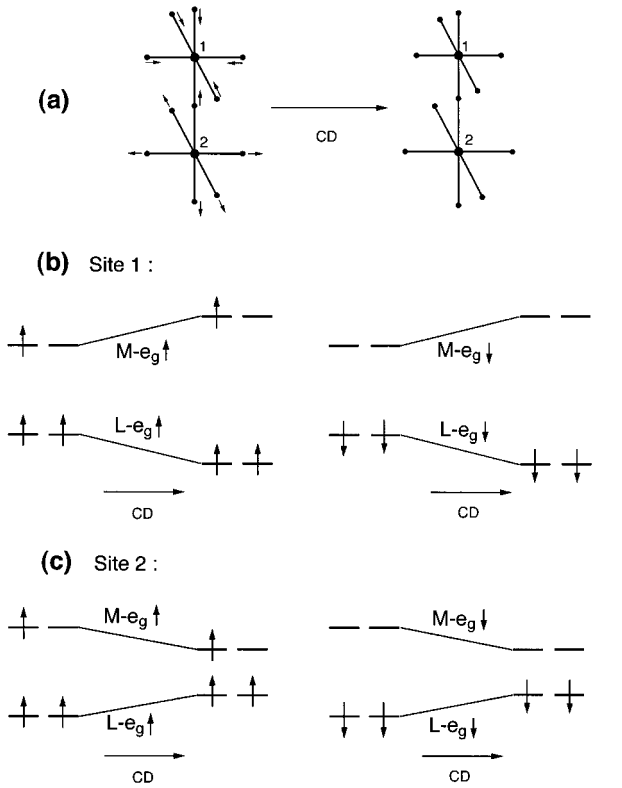

Figure 7. (a) Schematic representation of a CD distortion involving two adjacent MO_6 octahedra each containing a d^4 metal ion. (b) Effect of the CD distortion on the up- and down-spin L-e_g and M-e_g orbitals of the contracted site M(1). (c) Effect of the CD distortion on the up- and down-spin L-e_g and M-e_g orbitals of the expanded site M(2). Here the M(1) and M(2) sites are assumed to have a ferromagnetic spin arrangement.

$- y^2$) levels change by a JT distortion and neglecting the effect of the L-($3z^2 - r^2$) and L-($x^2 - y^2$) levels. A JT distortion is favored by the L-($x^2 - y^2$) level but is more strongly opposed by L-($3z^2 - r^2$) level. The opposing effect of the L-($3z^2 - r^2$) level would be stronger when the M−O bonding is more covalent. The driving force for the JT distortion would be strongly reduced in $CaFeO_3$ because the L-($3z^2 - r^2$)↑ level is strongly covalent in $CaFeO_3$.

Figure 7a depicts an ideal CD in which all the M−O bonds of an MO_6 octahedron are decreased at one metal site, M(1), but increased in the adjacent metal site, M(2). At the contracted site M(1), the CD raises the M-e_g levels but lowers the L-e_g levels (Figure 7b). At the expanded site M(2), the opposite is found (Figure 7c). (Here, for simplicity, the two iron sites M(1) and M(2) are assumed to have a ferromagnetic arrangement.) The overlap between the M 3d and O 2p orbitals increases exponentially with decreasing the M−O distance. Consequently, the extent of the energy level change should be larger at the contracted site M(1) than at the expanded site M(2). Therefore, unless the electron in the raised energy level, M-$e_g\uparrow$, of M(1) is transferred to a low-lying empty level of M(1) or M(2), the CD cannot lead to overall stabilization. The low-lying empty levels that can accommodate the electron-transfer include the M-$e_g\uparrow$ level of M(2) as well as the M-$t_{2g}\downarrow$ levels of M(1) and M(2).

In section 2 we showed for the ideal cubic structure of $CaFeO_3$ that the Fermi level occurs in the middle of the M-$e_g\uparrow$ bands and at the bottom of the M-$t_{2g}\downarrow$ bands. In other words, for the FeO_6 octahedra of $CaFeO_3$, the M-$e_g\uparrow$ levels lie lower than, but are close to, the M-$t_{2g}\downarrow$ levels (Figure 8a). As depicted in Figure 8b,c, let us suppose that at the contracted M(1) site the M-$e_g\uparrow$ levels are raised above the M-$t_{2g}\downarrow$ levels while at the expanded M(2) site the M-$e_g\uparrow$ levels are lowered, and neglect small differences in the t_{2g} levels of the M(1) and M(2) sites for simplicity (see below). Then an electron transfer from the M-$e_g\uparrow$ levels of M(1) to the M-$t_{2g}\downarrow$ levels

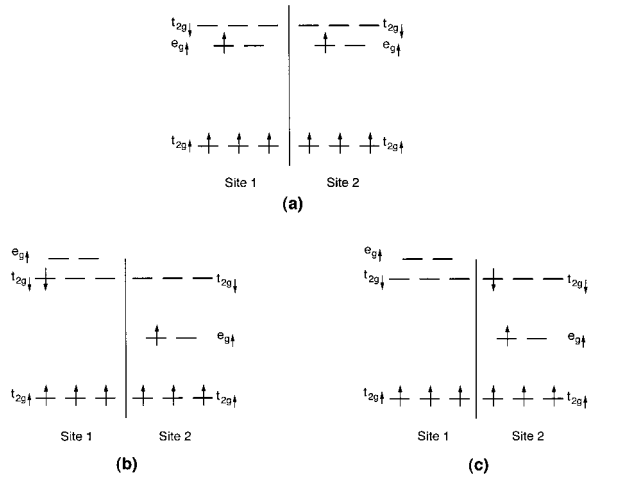

Figure 8. Schematic diagrams showing the relative orderings of the metal $t_{2g}\uparrow$, $t_{2g}\downarrow$ and $e_g\uparrow$ levels of the Fe(1) and Fe(2) sites in $CaFeO_3$: (a) in the absence of CD in which the Fe(1) and Fe(2) sites are equivalent; (b, c) in the presence of CD in which the Fe(1) site is contracted and the Fe(2) site is expanded. For simplicity, the $t_{2g}\uparrow$ and $t_{2g}\downarrow$ levels of the Fe(1) and Fe(2) sites were taken to be the same in (b) and (c).

of M(1) generates the configuration Ψ_1 (Figure 8b).

$$\Psi_1 = [(\text{M-}t_{2g}{}^{\uparrow})^3(\text{M-}t_{2g}{}^{\downarrow})^1]_{\text{site}-1}[(\text{M-}t_{2g}{}^{\uparrow})^3(\text{M-}e_g{}^{\uparrow})^1]_{\text{site}-2} \quad (4a)$$

$$\Psi_2 = [(\text{M-}t_{2g}{}^{\uparrow})^3]_{\text{site}-1}[(\text{M-}t_{2g}{}^{\uparrow})^3(\text{M-}e_g{}^{\uparrow})^1(\text{M-}t_{2g}{}^{\downarrow})^1]_{\text{site}-2} \quad (4b)$$

Consider the electron transfer from the M-$e_g{}^{\uparrow}$ level at the contracted site M(1) to the expanded site M(2). Then the resulting d^5 ion at the M(2) site might adopt the intermediate-spin configuration $(t_{2g}{}^{\uparrow})^3(t_{2g}{}^{\downarrow})^1(e_g{}^{\uparrow})^1$ or the high-spin configuration $(t_{2g}{}^{\uparrow})^3(e_g{}^{\uparrow})^2$. An analysis similar to that given in section 3 shows that the intermediate-spin configuration is more stable than the high-spin configuration if $10Dq > 2K_{dd}$. This would be the case for an octahedral ion, for which $10Dq$ is large. Therefore, the electron transfer from the M(1) to the M(2) site will lead to the configuration Ψ_2 (Figure 8c).

If the two configurations Ψ_1 and Ψ_2 contribute equally to the CD state, the M(1) and M(2) sites will have the spin magnetic moments of 2.5 and 3.5 μ_B, respectively. This prediction is in agreement with the finding that the low-temperature magnetic data of $CaFeO_3$ are well fit by a screw spiral structure with Fe moments 2.5 and 3.5 μ_B.[6,11] The degree of CD, δ, increases gradually from 0 toward 1 as the temperature is lowered.[6,7,10,11] To gain insight into this observation, we examine how the temperature lowering affects the relative contributions of Ψ_1 and Ψ_2 to the CD. The Ψ_1 configuration involves no electron transfer from the M(1) to the M(2) site, so that only Ψ_1 contributes to the CD state of $\delta = 0$. The Ψ_2 configuration involves one electron transfer from the M(1) to the M(2) site, so that only Ψ_2 contributes to the CD state of $\delta = 1$. As mentioned above, the CD state of $CaFeO_3$ reached at low temperatures has nearly equal contributions from Ψ_1 and Ψ_2 and is therefore best described as the CD state of $\delta = 0.5$. This implies that as the temperature is lowered from room temperature, the contribution of Ψ_2 to the CD state is steadily increased eventually becoming as large as that of Ψ_1. Let us speculate why the relative contributions of Ψ_1 and Ψ_2 change gradually as described above. According to our discussion in section 3, the electron transfer from M(1) to M(2) would raise the orbital levels of M(2) due to the additional electron−electron repulsion brought about by the transferred electron. This makes the Ψ_2 configuration higher in energy than the Ψ_1 configuration, so that the weight of Ψ_2 becomes smaller than that of Ψ_1 in the CD state. However, the mean M−O distance of MO_6 octahedra decreases upon lowering the temperature and this enhances the raising of the d-block levels at the contracted site M(1). The latter raises the energy of the Ψ_1 configuration, hence reduces the effect of electron−electron repulsion, and eventually makes the Ψ_1 and Ψ_2 configurations equally important at low temperatures.

The above discussion suggests that, for a perovskite AMO_3 of high-spin d^4 ions and strongly covalent M−O bonds, the driving force for a cooperative JT distortion is reduced and a CD becomes an energetically more favorable distortion. $LaMnO_3$ favors a JT distortion because the covalent character of the Mn−O bond is weak while $CaFeO_3$ prefers a CD distortion because the covalent character of the Fe−O bond

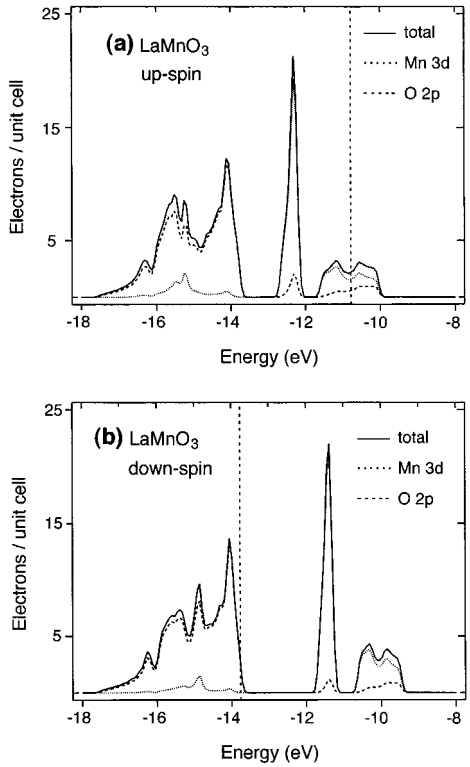

Figure 9. TDOS and PDOS plots calculated for the ideal cubic structure of $LaMnO_3$ by EHTB calculations: (a) decomposition of the up-spin TDOS (solid line) into the Mn 3d orbital (dotted line) and oxygen 2p orbital (dashed line) contributions, where the Fermi level represents that the e_g bands are half-filled; (b) decomposition of the down-spin TDOS (solid line) into the Mn 3d orbital (dotted line) and oxygen 2p orbital (dashed line) contributions, where the Fermi level represents the top of the oxygen p-block bands.

is strong. The CD of $CaFeO_3$ involves "bond disproportionation". In the absence of this "bond disproportionation", the high-spin $Fe^{4+}(d^4)$ ions of $CaFeO_3$ lead to a half-filled M-$e_g{}^{\uparrow}$ band thus making the high-temperature phase of $CaFeO_3$ metallic. Therefore, the CD of $CaFeO_3$ can also be viewed as a Peierls transition because the "bond disproportionation" opens an energy gap at the Fermi level (see the next section).

5. Computational Tests

We now test the suggestion of the previous section concerning how the covalent character of the M−O bond controls the JT distortion and CD of a perovskite AMO_3 on the basis of extended Hückel tight-binding (EHTB) electronic band structure calculations[24,25] for the ideal cubic and distorted structures of $LaMnO_3$ and $CaFeO_3$. First, it is necessary to find the atomic orbital parameters of EHTB calculations that bring out the essential features of the first principles electronic band structures calculated for the ideal cubic structures of $LaMnO_3$ and $CaFeO_3$ (Figures 2 and 3). As summarized in Figure 9 for $LaMnO_3$ and in Figure 10 for $CaFeO_3$, this is achieved by using the atomic parameters summarized in Table 1. The salient features of these EHTB calculations are as follows: (a) Double-ζ Slater type orbit-

(24) Whangbo, M.-H.; Hoffmann, R. *J. Am. Chem. Soc*. **1978**, *100*, 6093.
(25) Our calculations were carried out by employing the *CAESAR* program package (Ren, J.; Liang, W.; Whangbo, M.-H. *Crystal and Electronic Structure Analysis Using CAESAR*; 1998; http://www.PrimeC.com/).

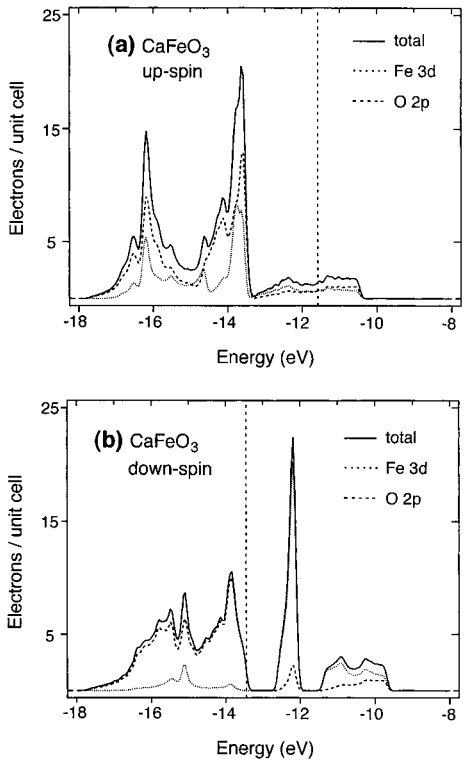

Figure 10. TDOS and PDOS plots calculated for the ideal cubic structure of $CaFeO_3$ by EHTB calculations: (a) decomposition of the up-spin TDOS (solid line) into the Fe 3d orbital (dotted line) and oxygen 2p orbital (dashed line) contributions, where the Fermi level represents that the e_g bands are half-filled; (b) decomposition of the down-spin TDOS (solid line) into the Fe 3d orbital (dotted line) and oxygen 2p orbital (dashed line) contributions, where the Fermi level represents the top of the oxygen p-block bands.

als[26] are used for the metal 3d and the oxygen 2s/2p orbitals. (b) Separate EHTB calculations were carried out for the up- and down-spin bands using different valence state ionization potentials (VSIP's) for the transition metal 3d level, with lower and higher VSIP values for the up- and down-spin bands, respectively. (c) The VSIP values of the Mn 3d, Fe 3d, and O 2p levels vary in the order

$$\text{O 2p} \approx \text{Fe 3d}(\uparrow) < \text{Fe 3d}(\downarrow) \approx \text{Mn 3d}(\uparrow) < \text{Mn 3d}(\downarrow) \quad (5)$$

This orbital sequence is accordance with the picture of how the degree of covalent character in the M−O (M = Mn, Fe) bond changes as a function of the energy difference between the metal 3d and oxygen 2p levels. The same atomic parameters are used for our EHTB calculations for the distorted structures of $LaMnO_3$ and $CaFeO_3$. Figure 11a,b summarizes the TDOS and PDOS plots of the up-spin and down-spin bands calculated for the 4.2 K structure of $LaMnO_3$,[4] which shows a JT distortion. Likewise, Figure 12a−d summarizes the TDOS and PDOS plots of the up-spin and down-spin bands calculated for the 15 K structure of $CaFeO_3$,[6] which has a CD distortion. In both $LaMnO_3$ and $CaFeO_3$ the distortion from the ideal cubic structure has a strong effect on the M-e_g bands, which are split by the distortion. We note for $CaFeO_3$ that the lower M-$e_g{\uparrow}$ bands have a larger contribution from the expanded Fe(2) site, and

(26) Clementi, E.; Roetti, C. *At. Data Nucl. Data Tables* **1974**, *14*, 177.

Table 1. Exponents ζ_i and Valence Shell Ionization Potentials H_{ii} of Slater-type Orbitals χ_i Used for Extended Hückel Tight-Binding Calculation[a]

atom	χ_i	H_{ii} (eV)	ζ_i	c_1[b]	ζ_i'	c_2[b]
Mn	4s	−6.60	1.844	1.0		
Mn	4p	−4.30	1.350	1.0		
Mn	3d	−12.7 (−11.7)[c]	5.767	0.3898	2.510	0.7297
Fe	4s	−6.80	1.925	1.0		
Fe	4p	−4.30	1.390	1.0		
Fe	3d	−14.6 (−12.6)[c]	6.068	0.4038	2.618	0.7198
O	2s	−32.3	2.688	0.7076	1.675	0.3745
O	2p	−14.8	3.694	0.3322	1.659	0.7448

[a] H_{ii}'s are the diagonal matrix elements $\langle\chi_i|H^{\text{eff}}|\chi_i\rangle$, where H^{eff} is the effective Hamiltonian. In our calculations of the off-diagonal matrix elements $H^{\text{eff}} = \langle\chi_i|H^{\text{eff}}|\chi_j\rangle$, the weighted formula was used.[28] [b] Coefficients used in the double-ζ Slater-type orbital expansion. [c] The lower value is used for the up-spin band calculations, and the higher value for the down-spin band calculations.

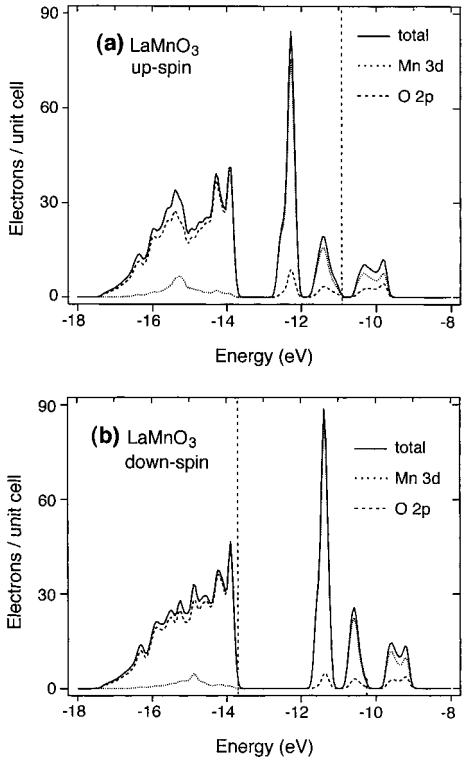

Figure 11. TDOS and PDOS plots calculated for the JT-distorted structure of $LaMnO_3$ by EHTB calculations: (a) decomposition of the up-spin TDOS (solid line) into the Mn 3d orbital (dotted line) and oxygen 2p orbital (dashed line) contributions, where the Fermi level represents that the e_g bands are half-filled; (b) decomposition of the down-spin TDOS (solid line) into the Mn 3d orbital (dotted line) and oxygen 2p orbital (dashed line) contributions, where the Fermi level represents the top of the oxygen p-block bands.

the upper M-$e_g{\uparrow}$ bands have a larger contribution from the contracted Fe(1) site (Figure 12b).

[In Figures 9−12 the Fermi level for the up-spin bands, $E_{f\uparrow}$, is placed to make the up-spin e_g bands half-filled, while the Fermi level for the down-spin bands, $E_{f\downarrow}$, is placed at the top of the oxygen p-block bands. When the up-spin and down-spin bands are shifted so as to make $E_{f\uparrow} = E_{f\downarrow}$, then the resulting electronic structure would become similar to that obtained from first principles spin-polarized electronic band structure calculations. However, to be consistent with our discussion about the CD of $CaFeO_3$ using the d-block levels of Figure 8b,c, the Fermi level $E_{f\uparrow}$ should be placed

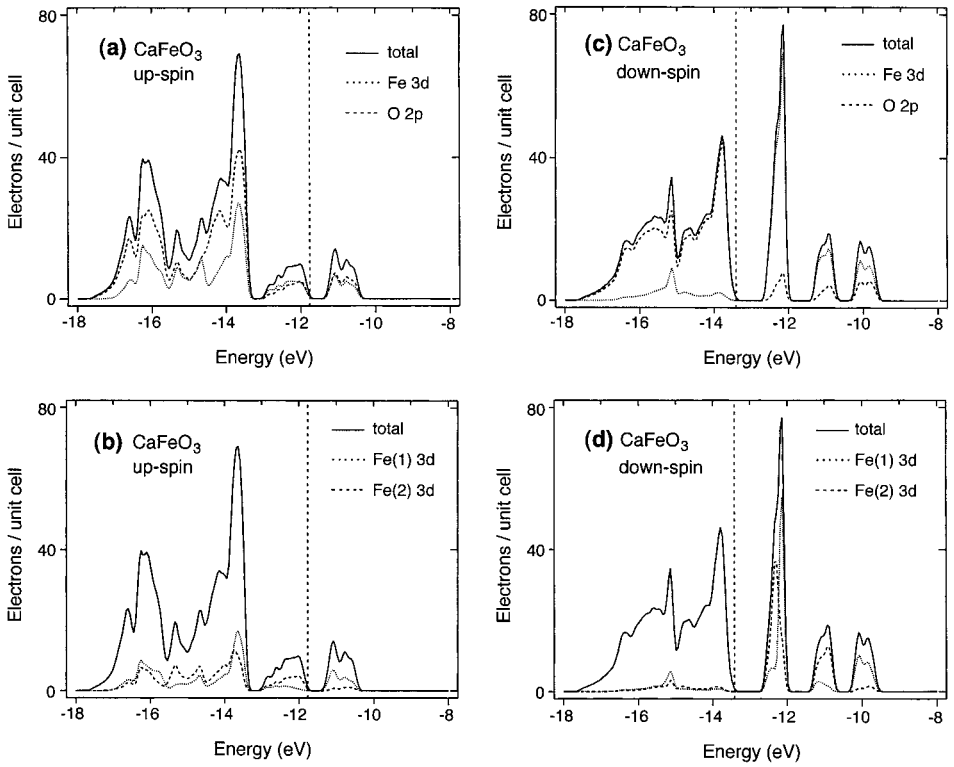

Figure 12. TDOS and PDOS plots calculated for the CD distorted structure of $CaFeO_3$ by EHTB calculations: (a) decomposition of the up-spin TDOS (solid line) into the Fe 3d orbital (dotted line) and oxygen 2p orbital (dashed line) contributions, where the Fermi level represents that the e_g bands are half-filled; (b) decomposition of the up-spin TDOS (solid line) into the Fe(1) 3d orbital (dotted line) and Fe(2) 3d orbital (dashed line) contributions, where the Fermi level represents that the e_g bands are half-filled; (c) decomposition of the down-spin TDOS (solid line) into the Fe 3d orbital (dotted line) and oxygen 2p orbital (dashed line) contributions, where the Fermi level represents the top of the oxygen p-block bands; (d) decomposition of the down-spin TDOS (solid line) into the Fe(1) 3d orbital (dotted line) and Fe(2) 3d orbital (dashed line) contributions, where the Fermi level represents the top of the oxygen p-block bands.

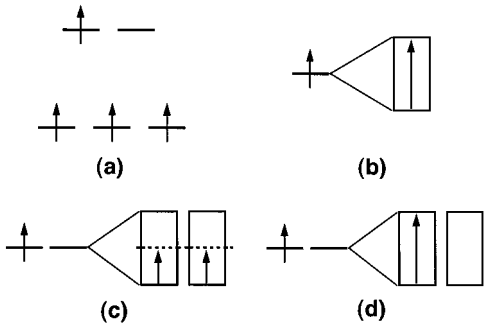

Figure 13. (a) Schematic representation of the high-spin d^4 configuration of a MO_6 octahedron. (b) Band filling leading to a magnetic insulating state (right) for a solid containing one orbital and one electron per repeat unit (left). (c) Band filling leading to a half-metallic state (right) for a solid containing two degenerate levels and one electron per repeat unit (left). (d) Band filling leading to a magnetic insulating state (right) for a solid containing two degenerate levels and one electron per repeat unit (left).

below the top of the lower M-$e_g\uparrow$ bands and the Fermi level $E_f\downarrow$ above the bottom of the M-$t_{2g}\downarrow$ bands.]

Let us estimate the energies of stabilization ΔE associated with the JT distortion in $LaMnO_3$ and the CD distortion in $CaFeO_3$ on the basis of our EHTB calculations. For this purpose, it is necessary to examine the meaning of the band occupancies of the cubic perovskite structures determined by electronic band structure calculations. The high-spin d^4 configuration of a MO_6 octahedron is represented as in Figure 13a. Our task is to identify the band occupancies of the ideal cubic perovskite AMO_3 that correspond to this local electron configuration. When a repeat site of a solid has one orbital and one electron, the band filling of its magnetic insulating state is given as shown in Figure 13b,[27] where all the band levels are singly filled. For a solid with two degenerate levels and one electron/repeat unit, spin-polarized electronic band structure calculations fill the resulting two up-spin bands as shown in Figure 13c, where each band is half-filled. It should be noted that such a representation has been used in our description of the up-spin e_g bands calculated for the ideal cubic structures of $LaMnO_3$ and $CaFeO_3$. The band filling of Figure 13c represents a half-metallic state, i.e., a metallic state in which the Fermi level cuts only one kind of spin bands (either up-spin or down-spin).[18] The alternative band filling shown in Figure 13d gives rise to a magnetic insulating state,[23] where all the levels of only one band are singly filled. We employ such a band filling of the up-spin e_g bands to represent the magnetic insulating states of the ideal cubic perovskites of $LaMnO_3$ and $CaFeO_3$.

Table 2 summarizes the total electronic energies (per formula unit in eV) calculated for the ideal cubic and distorted structures of $LaMnO_3$ and $CaFeO_3$ (i.e., the numbers without parenthesis). The stabilization energies ΔE (per formula unit in kcal/mol) associated with the distortions from the ideal cubic structures show that the JT distorted structure is more stable than the ideal cubic structure in $LaMnO_3$ and

(27) Whangbo, M.-H. *J. Chem. Phys.* **1979**, *70*, 4963.
(28) Ammeter, J.; Bürgi, H.-B.; Thibeault, J.; Hoffmann, R. *J. Am. Chem. Soc.* **1978**, *100*, 3686.

Table 2. Calculated Energies (per Formula Unit in eV) of the Ideal and Distorted Structures of $LaMnO_3$ and $CaFeO_3$ and Stabilization Energies ΔE (per Formula Unit in kcal/mol) Associated with the Distortions

structure	$LaMnO_3$[a]	$CaFeO_3$[b]
ideal	−515.38 (−523.58)	−522.97 (−514.49)
real	−515.91 (−523.75)	−523.60 (−514.95)
ΔE (kcal/mol)	−12.2 (−3.7)	−14.5 (−10.4)

[a] The numbers in parentheses were calculated by assuming that the Mn atom has the atomic parameters of Fe. [b] The numbers in parentheses were calculated by assuming that the Fe atom has the atomic parameters of Mn.

the CD structure is more stable than the ideal cubic structure in $CaFeO_3$. Our discussion of section 4 led to the suggestions that the Fe 3d orbital parameters generate more covalent bonding with oxygen than do the Mn 3d orbital parameters, that weak covalent bonding in the Mn−O bond makes $LaMnO_3$ undergo a JT distortion rather than a CD, and that strong covalent bonding in the Fe−O bond makes $CaFeO_3$ undergo a CD rather than a JT distortion. Consequently, if we were to calculate the electronic band structure of $LaMnO_3$ using the atomic orbital parameters that provide a stronger covalent bonding, the ΔE value should become smaller in magnitude. Likewise, if the electronic band structure of $CaFeO_3$ were calculated using the atomic orbital parameters that generate a weaker covalent bonding, the ΔE value should become smaller in magnitude. To test these predictions, we calculated the electronic band structures of $LaMnO_3$ assuming that the Mn atom has the atomic parameters of Fe and those of $CaFeO_3$ assuming that the Fe atom has the atomic parameters of Mn. As summarized in Table 2 (i.e., the numbers in parentheses), these calculations give less stabilization for each perovskite, in agreement with the suggestions.

6. Concluding Remarks

Spin-polarized electronic band structure calculations lead to different orbital compositions in the up- and down-spin bands of a given compound. This is caused by electron−electron repulsion, which greatly enhances the energy gap between the metal 3d and the oxygen 2p orbitals for the down-spin−orbital interactions but does not change it much for the up-spin−orbital interactions. Consequently, for both $LaMnO_3$ and $CaFeO_3$, the metal 3d orbital contribution is larger in the down-spin than in the up-spin d-block e_g bands. The driving force toward a cooperative JT distortion in a perovskite AMO_3 of high-spin d^4 cations is reduced when the M−O bond has a strong covalent character. For such a perovskite, a CD can become energetically more favorable than a JT distortion. $LaMnO_3$ prefers a JT distortion because a covalent character is weak in the Mn−O bond, while $CaFeO_3$ favors a CD distortion because a covalent character is strong in the Fe−O bond. The low-temperature magnetic data of $CaFeO_3$ is well fit by a screw spiral structure[6,11] with Fe moments 2.5 and 3.5 μ_B and also by an amplitude-modulated model with maximum amplitudes of 3.5 and 5.0 μ_B.[6] The driving force for a CD is the electron transfer from the M-$e_g^{\uparrow}$ level at the contracted site $Fe^{(4+\delta)+}$ to the M-$t_{2g}^{\downarrow}$ levels at the contracted site $Fe^{(4+\delta)+}$ and at the expanded site $Fe^{(4-\delta)+}$. This predicts the spin moments 2.5 and 3.5 μ_B for the $Fe^{(4+\delta)+}$ and $Fe^{(4-\delta)+}$ sites, respectively, and therefore supports the screw spiral model.

Acknowledgment. The work at North Carolina State University was supported by the Office of Basic Energy Sciences, Division of Materials Sciences, U.S. Department of Energy, under Grant DE-FG02-86ER45259. The computational work at ICMCB was aided by the M3PEC project (Modélisation Microscopique et Mésoscopique en Physique, dans l'Environnement et en Chimie), Université de Bordeaux I.

IC0110427